Functional Characterization and Mutation Analysis of Human ATP:Cob(I)alamin Adenosyltransferase†

Chenguang Fan and Thomas A. Bobik*

Department of Biochemistry, Biophysics and Molecular Biology, Iowa State University, Ames, Iowa 50011

Received July 25, 2007

ABSTRACT: ATP:cob(I)alamin adenosyltransferase catalyzes the final step in the conversion of vitamin B_{12} into the active coenzyme, adenosylcobalamin. Inherited defects in the gene for the human adenosyltransferase (hATR) result in methylmalonyl aciduria (MMA), a rare but life-threatening illness. In this study, we conducted a random mutagenesis of the hATR coding sequence. An ATR-deficient strain of *Salmonella* was used as a surrogate host to screen for mutations that impaired hATR activity *in vivo*. Fifty-seven missense mutations were isolated. These mapped to 30 positions of the hATR, 25 of which had not previously been shown to impair enzyme activity. Kinetic analysis and *in vivo* tests for enzyme activity were performed on the hATR variants, and mutations were mapped onto a hATR structural model. These studies functionally defined the hATR active site and tentatively implicated three amino acid residues in facilitating the reduction of cob(II)alamin to cob(I)alamin which is a prerequisite to adenosylation.

In higher animals, two cobalamin (B_{12})-dependent enzymes are known. Methylcobalamin-dependent methionine synthase (MS)[1] is needed for recycling homocysteine to methionine (*1, 2*), and adenosylcobalamin-dependent methylmalonyl-CoA mutase (MCM) is essential for the conversion of propionyl-CoA to the TCA cycle intermediate, succinyl-CoA (*3*). In higher animals, propionyl-CoA is produced from the breakdown of branched-chain amino acids as well as thymine, cholesterol, and odd-chain fatty acids. Hence, MCM is essential for the complete catabolism of these compounds (*3*).

Humans are incapable of synthesizing AdoCbl and MeCbl *de novo* and depend on assimilation of exogenous complex precursors such as vitamin B_{12} (cyanocobalamin, CN-Cbl) and hydroxycobalamin (OH-Cbl). For AdoCbl synthesis, CN-Cbl is converted to OH-Cbl, successively reduced to cob(II)alamin and cob(I)alamin, and finally adenosylated to AdoCbl (*4–6*). For MeCbl synthesis, cob(II)alamin is reductively methylated while bound to MS (*2, 7, 8*). In humans, inherited defects in the genes for MCM (mut), MS (MTR), or the genes for cobalamin metabolism lead to methylmalonyl aciduria (MMA), homocystinuria, or combined disease (*9, 10*). Patients typically present within the first year of life with lethargy, failure to thrive, recurrent vomiting, dehydration, respiratory distress, and hypotonia and are prone to life-threatening acidosis (*11*).

The final step in the conversion of vitamin B_{12} to AdoCbl is catalyzed by ATP:cob(I)alamin adenosyltransferase (ATR) (*5, 12*). Three families of ATRs that are unrelated in amino acid sequence have been identified: CobA type, PduO type, and EutT type (*13–16*). The human adenosyltransferase (hATR) is a PduO-type enzyme (*17*). The gene for hATR is MMAB, and defects in this gene underlie the cblB complementation group of isolated MMA (*18*). The crystal structures of the hATR and two related bacterial enzymes from *Lactobacillus reuteri* and *Thermoplasma acidophilum* were recently determined (*19–21*). These enzymes are trimers, where the monomer is a five-helix bundle and the active site is at the subunit interface. The structures of the human and *L. reuteri* enzymes were determined with MgATP bound which identified a unique ATP-binding motif (*19, 20*). These studies also showed that binding of MgATP increased the order of 20 N-terminal amino acids, creating a novel MgATP binding site that is part of a larger cleft proposed to include the cobalamin binding site. Thus far, a structure of a PduO-type ATR with cobalamin bound has not been reported, although a structure for a CobA-type ATR with cobalamin bound is available (*22*).

Recent spectroscopic studies indicate that in the presence of MgATP, hATR binds cob(II)alamin in a four-coordinate form in which dimethylbenzimidizole (DMB) is not coordinated to the cobalt in contrast to cob(II)alamin in solution at physiological pH where DMB is the lower axial ligand to cobalt (*23*). Dissociation of DMB changes the redox potential for the cob(II)alamin/cob(I)alamin couple from −610 mV to approximately −500 mV (*24*), and this increase in potential is proposed to facilitate cob(II)alamin reduction *in vivo* (*25*). In addition to preferentially binding cob(II)alamin in a DMB-off form, the hATR also binds AdoCbl DMB-off which may facilitate coenzyme transfer to MCM which binds

† This work was supported by National Institutes of Health Grant DK064771 to T.A.B.

* To whom correspondence should be addressed: Department of Biochemistry, Biophysics and Molecular Biology, Iowa State University, Ames, IA 50011. Phone: (515) 294-4165. Fax: (515) 294-0453. E-mail: bobik@iastate.edu.

[1] Abbreviations: ATR, ATP:cob(I)alamin adenosyltransferase; hATR, human adenosyltransferase; MeCbl, methylcobalamin; MS, methionine synthase; AdoCbl, adenosylcobalamin; MCM, methylmalonyl-CoA mutase; CN-Cbl, cyanocobalamin; OH-Cbl, hydroxycobalamin; MMA, methylmalonyl aciduria; DMB, dimethylbenzimidizole; DTT, dithiothreitol; IPTG, isopropyl β-D-thiogalactopyranoside; LB, Luria-Bertani; SDS−PAGE, sodium dodecyl sulfate−polyacrylamide gel electrophoresis; MTS, mitochondrial targeting sequence; EPR, electron paramagnetic resonance.

10.1021/bi800084a CCC: $40.75
Published on Web 02/06/2008

cobalamin with H626 replacing DMB as the lower ligand to cobalt (*25*).

Studies with the hATR and the CobA and PduO ATRs from *Salmonella* indicate that these enzymes closely interact with partner reductases and that cob(I)alamin is not produced free in solution but rather exists as an enzyme-bound species that is rapidly adenosylated to AdoCbl (*26–28*). It has been proposed that this is essential to prevent byreaction of cob(I)alamin which is one of the strongest nucleophiles known in biology (*29*). Mechanistic studies of the PduO enzyme of *Salmonella* indicate a ternary complex mechanism rather than a substituted enzyme mechanism (*30*). Cumulatively, the studies mentioned above lead to a general model for ATR function in which MgATP binds first followed by cob(II)alamin and cobalamin reductase. Subsequently, cob(II)alamin is reduced to cob(I)alamin which is adenosylated to AdoCbl.

To date, relatively little work has been reported that describes how amino acid changes affect the activity of PduO-type ATRs such as the human enzyme. The effects of four amino acid changes (R186W, R190H, R191W, and E193K) on hATR activity were determined, and three of the four corresponding amino acid residues were also studied in the *Thermoplasma* enzyme (*21, 31*). No general study on the effects of mutations on hATR activity and function has been reported. Therefore, we conducted a random mutagenesis of the hATR using *Salmonella* as a surrogate host to screen for changes in enzyme activity *in vivo*. Fifty-seven missense mutations at 30 positions were found to impair hATR activity *in vivo* in the surrogate host. These included mutations at 25 new sites that eliminate or reduce the hATR activity and hence could result in MMA if found in humans. In addition, we performed kinetic analysis and *in vivo* tests for enzyme activity on the hATR variants and mapped the mutations isolated onto a hATR structural model. These studies functionally defined the hATR active site and tentatively indicate a role for three amino acid residues in facilitating cob(II)alamin reduction by mediating the DMB-off transition.

MATERIALS AND METHODS

Chemicals and Reagents. Dithiothreitol (DTT), OH-Cbl, and AdoCbl were purchased from Sigma (St. Louis, MO). Titanium(III) citrate was prepared as described previously (*32*). Isopropyl β-D-thiogalactopyranoside (IPTG) was from Diagnostic Chemical Ltd. (Charelottetown, PE). Restriction enzymes and T4 DNA ligase were from New England Biolabs (Beverly, MA). Pefabloc SC PLUS was purchased from ICN Biomedicals, Inc. (Aurora, OH). Other chemicals were from Fisher Scientific (Norcross, GA).

Bacterial Strains, Media, and Growth Conditions. The bacterial strains used in this study are listed in Table 1. The minimal medium used was NCE supplemented with 0.4% 1,2-propanediol (1,2-PD), 1 mM $MgSO_4$, 200 ng/mL OH-B_{12}, and 3 mM (each) valine, isoleucine, leucine, and threonine. LB (Luria-Bertani) medium was the rich medium used. MacConkey-1,2-PD-OH-Cbl indicator plates were composed of MacConkey agar base (Difco, Detroit, MI) supplemented with 1% 1,2-PD and 200 ng/mL OH-Cbl.

General Molecular and Protein Methods. Bacterial transformation, PCR, restriction enzyme digests, and other standard molecular and protein methods were performed as described previously (*13, 33*).

Table 1: Bacterial Strains Used in This Study

strain	genotype
Escherichia coli	
DH5α	F$^-$ λ^- *endA1 hsdR17 relA1 supE44 thi-1 recA1 gyrA96 relA1*Δ*(lacZYA-argF)U169* (φ80d*lacZ*ΔM15)
BL21DE3 RIL	F$^-$*ompT hsdS*(r_B^- m_B^-) *dcm*$^+$ Tet^r *gal*λ(DE3) *endA*Hte [*argU ileY leuW*Cam^r]
XL-1 Red	*endA*1 *gyrA*96 *thi*-1 *hsdR*17 *supE*44 *relA*1 *lac mutD*5*mutS mutT* Tn10 (tet^r)[a] (bought from Stratagene)
BE119	BL21DE3 RIL/pTA925 (T7 expression vector without insert)
BE260	DH5α/pNL166 (pLac22-hATR)
BE702	BL21DE3 RIL/pCF13 (His_8-hATR)
BE704	BL21DE3 RIL/pCF15 (hATR-His_8)
BE706	BL21DE3 RIL/pCF19 (native hATR)
Salmonella enterica serovar Typhimurium LT2	
BE121	Δ*pduO*651 *cobA*366::Tn10dCam
BE620	Δ*pduO*651 *cobA*366::dCam Δ1955 (zfa3646*Tn*10*zfa3648)
BE701	BE620/pCF13 (His_8-hATR)
BE703	BE620/pCF15 (hATR-His_8)
BE705	BE620/pCF19 (native hATR)
BE707	BE620/pCF (modified pTA925)

Cloning of the hATR Coding Sequence for High-Level Expression and Complementation of ATR-Deficient Salmonella. PCR was used to amplify the hATR coding sequence. Primers were chosen that remove the predicted 36-amino acid N-terminal mitochondrial targeting sequence (MTS). Plasmid pNL166 provided the template DNA (*17*). The primers used for amplification were 5′-GCC GCC AGA TCT TAT GCC TCA GGG CGT GGA AGA CGG G-3′ (forward) and 5′-GCC GCC AAG CTT ATC AGA GTC CCT CAG ACT CGG CCG-3′ (reverse) for native hATR. Primer 5′-GCC GCC AGA TCT TAT GCA CCA TCA CCA TCA TCA CCA CCA TCC TCA GGG CGT GGA GAC GGG-3′ was used to introduce an N-terminal His_8 tag, and primer 5′-GCC GCC AAG CTT ATC AAT GGT GGT GAT GAT GGT GAT GGT GGA GTC CCT CAG ACT CGG CCG-3′ was used to introduce a C-terminal His_8 tag. These primers also introduced *Bgl*II and *Hin*dIII restriction sites into the PCR products which were used for cloning into pTA925 restricted with *Bgl*II and *Hin*dIII. Ligation mixtures were used to transform *E. coli* DH5α by electroporation, and transformants were selected on LB medium containing 25 μg/mL kanamycin. Plasmid DNA was purified from these strains, and the DNA sequence of each clone was determined. Clones with the expected DNA sequence were restricted with *Sph*I and *Xba*I and ligated with a linker having the sequence 5′-CAA TTA ATA CGA CTC ACT ATA GAC CCC AGG CTT GAC ACT TTA TGC TTC CGG CTC TAT AAT GTG TGG AAT TGT GAG CGG T-3′ and 5′-CTA GAC CGC TCA CAA TTC CAC ACA TTA TAG AGC CGG AAG CAT AAA GTG TCA AGC CTG GGG TCT ATA GTG AGT CGT ATT AAT TGC ATG-3′. Ligation mixtures were

used to transform *E. coli* DH5α by electroporation. Transformants were selected on LB medium with 25 μg/mL kanamycin. Plasmid DNA was purified from these strains, and the DNA sequence of the linker region was verified. The linker introduced both *E. coli* and T7 promoters which allowed high-level protein production in BL21DE3 RIL as well as complementation of the ATR-deficient *Salmonella* strain used for identification of hATR mutations.

Growth of hATR Expression Strains and Preparation of Cell Extract. The *E. coli* strains used for expression of hATR were grown on 400 mL of LB supplemented with 25 μg/mL kanamycin at 16 °C in a New Brunswick Scientific Innova 4230 refrigerated shaker incubator with a shaking speed at 275 rpm. Cells were grown to an absorbance of 0.6–0.8 at 600 nm, and protein expression was induced by the addition of 0.5 mM IPTG. Cells were incubated at 16 °C with shaking at 275 rpm for an additional 18 h. Cells were removed from the incubator, held on ice for 10 min, and then harvested by centrifugation at 8000 rpm for 5 min using a Beckman JA-10 rotor. The cells were resuspended in 10 mL of 50 mM Tris and 300 mM NaCl (pH 7.5) and broken using a French pressure cell (Thermo Electron Corp.) at 10000 psi. Pefabloc SC PLUS was added to the cell extract to a concentration of 100 μg/mL to inhibit proteases. The crude cell extract was centrifuged at 16000 rpm for 30 min using a Beckman JA-17 rotor to separate the soluble and insoluble fractions. The supernatant was the soluble fraction used for enzyme purification.

Western Blots. The soluble fractions of cell extracts were fractionated by 12% SDS−PAGE and transferred onto a nitrocellulose membrane (Bio-Rad). The membrane was incubated at room temperature with gentle shacking in 50 mM Tris (pH 7.4), 200 mM NaCl, 0.1% Tween (TTBS), and 5% Milk blocking buffer for 30 min. The primary antibody used was the affinity-purified rabbit IgG anti-hATR diluted 1:1000. The secondary antibody was the goat anti-rabbit IgG (H+L) alkaline phosphatase conjugate (Bio-Rad) at a 1:3000 dilution. The membrane was prepared for detection using the alkaline phosphatase conjugate substrate kit (Bio-Rad).

ATP:Cob(I)alamin Adenosyltransferase Assays. ATR assays were performed as previously reported with some modifications (*30*). Reaction mixtures contained 200 mM Tris-HCl (pH 8.0), 5 mM $MgCl_2$, 10 mM KCl, 0.05 mM OH-Cbl, 0.5 mM ATP, and 1 mM titanium(III) citrate in a total volume of 2 mL. Reaction components (except for hATR) were dispensed into cuvettes inside an anaerobic chamber (Coy Laboratories, Grass Lake, MI). The cuvettes were sealed, removed from the chamber, and incubated at 37 °C for 5 min. Reactions were initiated by addition of purified recombinant hATR, and AdoCbl formation was assessed by following the decrease in absorbance at 388 nm ($\epsilon_{388} = 24.9\ cm^{-1}\ mM^{-1}$).

Random Mutagenesis and Screening of Candidate Human ATR Mutants. Random mutagenesis of the hATR gene was carried out using the *E. coli* mutator strain XL1-Red (Stratagene). pCF13 (His_8-hATR) and pCF15 (hATR-His_8) were transformed into XL1-Red by chemical transformation selecting for kanamycin resistance on LB medium. Approximately 3000 transformants were pooled and subcultured 5–10 times in 100 mL of LB medium inoculated with 0.5 mL of a LB culture. pCF13 and pCF15 DNA was purified and used to transform the ATR-deficient bacterial mutant BE620 via electroporation. Transformants were screened on MacConkey-1,2-PD-OH-Cbl indicator plates supplemented with kanamycin at 25 μg/mL.

Growth Tests. AdoCbl-dependent growth on 1,2-PD minimal medium was performed as previously described in 48-well microtiter plates (*13, 17*).

UV–Visible Spectroscopy for Examination of the Lower Axial Ligand of AdoCbl. Spectra were obtained using a Cary 50 Bio spectrophotometer (Varian). One milliliter of soluble cell extract containing 10 mg of protein was added to a 1 mL plastic cuvette, and the mixture was scanned from 300 to 600 nm as the baseline. Then, 2 μL of 5 mM AdoCbl (finally 5 μM) was added to the sample and gently mixed. After incubation at 37 °C for 2 min, the cuvette was scanned a second time from 300 to 600 nm.

EPR Spectroscopy for Examination of the Lower Axial Ligand of Cob(II)alamin. Spectra were obtained using Bruker ER-200 EPR system. Cob(II)alamin was generated by photolysis of AdoCbl under anaerobic conditions in 10 mM Tris-HCl (pH 8.0). Purified hATR (2 mM) was incubated with 2 mM ATP anaerobically for 20 min at 4 °C. Then, cob(II)alamin was added to a final concentration of 100 μM. The mixture was equilibrated for 5 min at 37 °C and then injected into 4 mm quartz EPR tubes.

DNA Sequencing. DNA sequencing was carried out by Iowa State University, at the DNA facility of the Iowa State University Office of Biotechnology.

RESULTS

An in Vivo Screen for hATR Mutants. Wild-type *Salmonella* produces red colonies on MacConkey-1,2-PD-B_{12} indicator media as a result of AdoCbl-dependent 1,2-PD degradation (*34*). *Salmonella* strain BE620 produces white colonies on similar media due to ATR deficiency (*13*). The phenotype of BE620 was complemented by pCF13 (His_8-hATR) or pCF15 (hATR-His_8), but not by a plasmid without an insert (data not shown). Hence, pCF13 or pCF15 with a hATR inactivated by mutation was expected to produce white or pink colonies in BE620 rather than wild-type red, providing a convenient *in vivo* screen for hATR mutants.

E. coli mutator strain XL1-Red was used for random mutagenesis of pCF13 (His_8-hATR) and pCF15 (hATR-His_8). Mutagenized plasmid DNA was transformed into the ATR-deficient bacterial mutant *Salmonella* BE620, and resultant colonies were screened for color formation on MacConkey-1,2-PD-B_{12} indicator media. Approximately 6000 transformants were screened, 3000 derived from each mutagenized plasmid. Of these, 185 produced colonies that were white or pink in color, suggesting that they carried a mutant hATR coding sequence. These included 57 single-base change missense mutations at 30 positions of the hATR gene with K78 and G97 each having two different mutations.

Effect of B_{12} Concentration on the Activity of hATR Variants in Vivo. We also used indicator plates with different amounts of OH-Cbl to view the sensitivity of the mutants to B_{12} concentration. Eleven mutants, G63E, D64G, R76G, K78R, G97R, G97E, S126L, H183Y, R215K, D218N, and R225K, had an increased level of color formation (ATR activity) at 1500 nM compared to 150 nM OH-Cbl. Of these amino acid residues, G63 and K78 directly contact MgATP

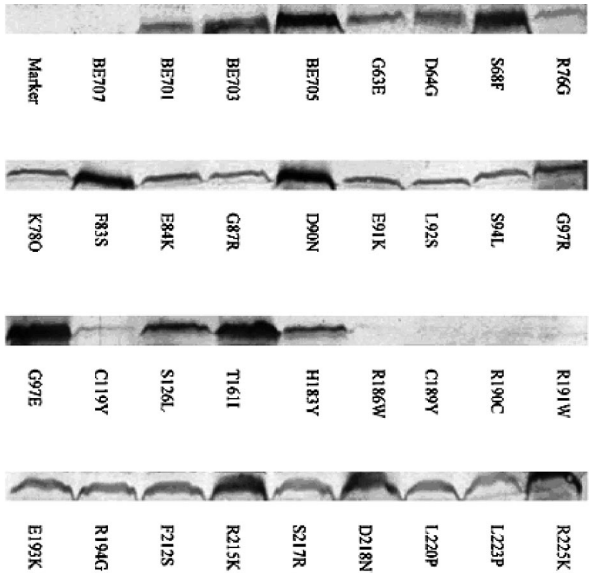

FIGURE 1: Western blotting analysis of hATR mutants. All lanes were loaded with 10 μg of soluble cell extract. The following strains were used: strain BE707 (no insert control), strain BE701 (His_8-hATR), strain BE703 (hATR-His_8), and strain BE705 (native hATR).

in the structural model, and residues D64, R76, S126, R215, D218, and R225 are at the surface of the proposed active site pocket in position to interact with MgATP or cobalamin. Thus, these results indicate that residues G63, D64, R76, K78, S126, R215, D218, and R225 are important to binding of MgATP/cobalamin by the hATR *in vivo*.

Results also showed that most of the mutants that were partly corrected by the increased B_{12} concentration had an elevated K_m for MgATP, cobalamin, or both substrates. This finding is consistent with the proposal that MgATP and cobalamin binding are interrelated which was indicated by structural studies that showed MgATP binding leads to ordering of the N-terminal portion of the hATR with formation of a proposed cobalamin-binding site (*19*).

We also found that two hATR mutations that are partly corrected by increased B_{12} levels *in vivo* (R215K and R225K) lack measurable activity *in vitro*, and two other B_{12}-sensitive mutations (G97R and H183Y) are at the inner part of the protein distant from the active site. Apparently, the R215K and R225K mutants are stabilized somewhat by the *in vivo* milieu, and G97R and H183Y affect the shape of the active site at a distance.

In Vivo Stability of hATR Mutants. The stability of the mutant hATR proteins in *Salmonella* BE620 was examined by Western blotting (Figure 1). Each lane contains 10 μg of protein. From these gels, it can be seen that most of the mutant hATRs were expressed at a level within 2-fold of the control. However, mutant proteins C119Y, R186W, C189Y, R190C, and R191W were produced at much lower levels than the control, indicating that these mutations impair proper protein folding leading to degradation by cellular proteases. Most of the unstable mutants are located in a highly conserved region of the hATR, and three of five have been found in MMA patients (*18*).

B_{12}-Dependent Growth of hATR Mutants in a Surrogate Host. Ectopic expression of His_8-hATR, hATR-His_8, or native hATR in ATR-deficient *Salmonella* restored AdoCbl-dependent growth on 1,2-PD which was previously shown

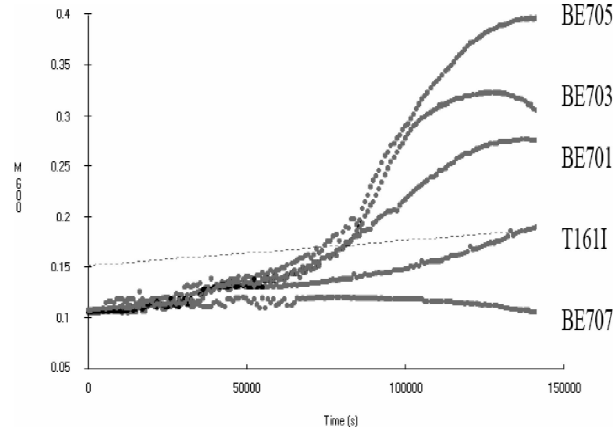

FIGURE 2: Growth tests with hATR mutants using *Salmonella* as a surrogate host. The following strains were used: BE701 (His_8-hATR), BE703 (hATR-His_8), BE705 (native hATR), and BE707 (no insert control). The mutants were grown on minimal medium with 1,2-PD as the only carbon source at 37 °C with shaking for 40 h. Cell growth was assessed by measuring OD_{600}. The control strain containing plasmid without insert (BE707) was unable to grow on 1,2-PD-B_{12} minimal medium due to a lack of ATR activity.

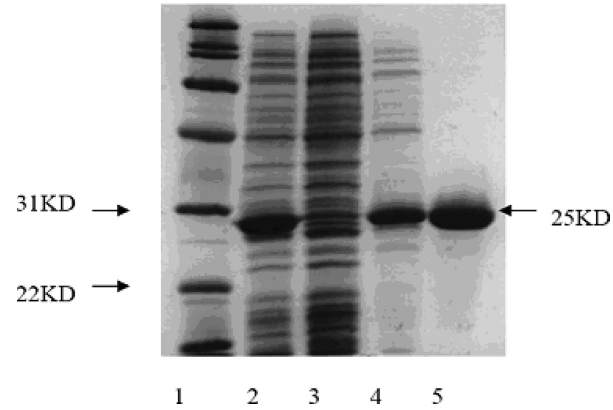

FIGURE 3: SDS−PAGE analysis of hATR-His_8 purification: lane 1, molecular mass markers; lane 2, 10 μg of soluble extract of strain BE704 (hATR-His_8); lane 3, 10 μg of flow-through fraction; lane 4, 5 μg of 80 mM imidazole wash fraction; and lane 5, 5 μg of 250 mM imidazole elution fraction. The molecular mass of hATR-His_8 is 25 kDa. The gel contained 12% acrylamide. Similar results were obtained for purification of His_8-hATR and the hATR mutants (data not shown).

with native hATR (*13*) (Figure 2). Although the growth rate obtained via ectopic expression of His_8-ATR was approximately half of that with native hATR or hATR-His_8, it was still much higher than the control; hence, we were able to further evaluate the *in vivo* activity of all hATR mutants with growth studies. With one exception (T161I), none of the hATR missense mutants enhanced the growth of ATR-deficient *Salmonella* BE620 on 1,2-PD. The T161I mutant was capable of slow growth. These results indicate that the 32 hATR missense mutants isolated here had little to no ATR activity *in vivo* when *Salmonella* was used a surrogate host.

Kinetic Values for Human ATR Mutants. Using purified enzymes (Figure 3), kinetic constants were determined for the wild-type and mutant hATRs. K_m and k_{cat} values were determined by nonlinear regression with Grafit (Table 2). When the K_m values for ATP were determined, saturating levels of cob(I)alamin (50 μM) were added to assay mixtures and the ATP concentration was varied from 0 to 200 μM. Similarly, saturating levels of ATP (500 μM) and varying

Table 2: Kinetic Constants for hATR Variants[a]

	K_{mATP} (μM)	$K_{mcob(I)}$ (μM)	k_{cat} (min^{-1})	k_{cat}/K_{mATP} (μM^{-1} min^{-1})	$k_{cat}/K_{mcob(I)}$ (μM^{-1} min^{-1})
His_8-hATR	7.19 ± 0.10	1.58 ± 0.65	2.77 ± 0.27	0.39	1.75
hATR-His_8	7.35 ± 0.67	1.60 ± 0.44	4.96 ± 0.26	0.67	3.10
native hATR	6.90 ± 0.36	1.60 ± 0.55	4.75 ± 0.23	0.69	2.97
G63E	12.4 ± 1.2	2.24 ± 0.60	0.49 ± 0.03	0.039	0.22
D64G	20.5 ± 2.8	1.94 ± 0.64	0.53 ± 0.04	0.026	0.27
S68F	17.2 ± 2.8	1.86 ± 0.55	0.78 ± 0.05	0.045	0.42
R76G	45.9 ± 8.2	9.09 ± 1.89	2.58 ± 1.20	0.056	0.28
K78R	8.26 ± 0.68	2.25 ± 0.35	0.32 ± 0.05	0.039	0.14
F83S	215 ± 37	30.2 ± 12.5	2.07 ± 1.58	0.010	0.07
G97R	20.3 ± 8.4	3.03 ± 0.62	0.80 ± 0.06	0.039	0.26
G97E	5.23 ± 1.25	2.52 ± 0.79	2.38 ± 0.13	0.46	0.94
C119Y	14.1 ± 1.7	5.13 ± 1.82	4.06 ± 0.30	0.29	0.79
S126L	87.7 ± 41	14.3 ± 4.5	0.58 ± 0.08	0.007	0.04
T161I	5.00 ± 0.91	2.71 ± 0.25	2.29 ± 0.05	0.46	0.85
H183Y	9.97 ± 2.01	7.13 ± 1.06	2.83 ± 0.43	0.28	0.40
D218N	2.87 ± 0.40	1.72 ± 0.43	0.73 ± 0.02	0.25	0.42

[a] Mean values were used to calculate k_{cat}/K_m. Mutants without measurable ability are not shown in this table.

levels of cob(I)alamin from 0 to 50 μM were used to determine the K_m values for cob(I)alamin.

Controls showed that hATR-His_8 and native hATR had similar activity. The N-terminal His_8 tag enzyme had a lower k_{cat} value (58%), showing that the N-terminal tag affected enzyme activity somewhat. Kinetic analysis of the hATR missense mutants indicated four distinct groups.

Group I consisted of 19 mutants (K78Q, E84K, G87R, D90N, E91K, L92S, S94L, R186W, C189Y, R190C, R191W, E193K, R194G, F212S, R215K, S217R, L220P, L223P, and R225K) that had no activity even with a 10-fold excess of ATP and cob(I)alamin compared to the standard assay (*13*). Most of these had mutations that changed conserved amino acid residues (*17*). Among these, R186W, R190C, R191W, and E193K have been found in methylmalonic aciduria patients (*18*). Note that although R186W, C189Y, R190C, and R191W were unstable when expressed in ATR-deficient *Salmonella* BE620 at moderate levels (Figure 1), it was still possible to purify these proteins following high-level expression in *E. coli* BL21DE3 RIL.

Group II consisted of three mutants that exhibited relatively large changes in the K_m values for both ATP and cob(I)alamin: R76G, F83S, and S126L. Their K_m values for ATP were 45.89 ± 8.17, 215 ± 37, and 87.70 ± 40.98 μM, respectively, while the wild-type value was 6.90 ± 0.36 μM. K_m values for cob(I)alamin were 9.09 ± 1.89, 30.2 ± 12.5, and 14.25 ± 4.49 μM, respectively, while the wild-type value was 1.60 ± 0.55 μM. Residue F83 has direct contact with MgATP in the crystal structure, and R76 and S126 map to the surface of the active site pocket. Hence, these residues are likely critical for proper binding of MgATP and/or cobalamin.

Group III mutants (G63E, D64G, S68F, K78R, G97R, and D218N) showed modest changes or wild-type K_m values for ATP and cob(I)alamin, but a substantially reduced V_{max}. Three of these residues interact directly with MgATP (G63, S68, and K78), and the remainder of the residues (D64, G97, and D218) map to the surface of the proposed active site pocket. Hence, these amino acid residues likely define the enzyme active site.

Group IV mutants (G97E, C119Y, T161I, and H183Y) had kinetic constants in the wild-type range. This raises the question of why these mutants were inactive in *Salmonella* *in vivo*. Western blots showed that hATR-C119Y was produced only at a low level *in vivo* (Figure 1); hence, it may have been inactive *in vivo* due to instability. However, the G97E, T161I, and H183Y hATR variants were all produced at near wild-type levels *in vivo*. We speculate that these mutations interfere with the reduction of cob(II)alamin to cob(I)alamin *in vivo* and thereby impair hATR activity. For the *in vitro* assay, cob(I)alamin is provided by use of a strong chemical reductant Ti(III); hence, a defect that impairs the reduction of cob(IIalamin) to cob(I)alamin would not be detected by this test.

Effect of Mutations on AdoCbl Binding. Prior studies showed that binding of AdoCbl to native hATR results in a large blue shift in its UV–visible spectrum from 540 to 460 nm because AdoCbl is bound base-off (without DMB as the lower axial ligand to cobalt) (*25*). It was proposed that this mode of binding allows efficient transfer of AdoCbl to MCM which binds AdoCbl in the base-off mode with H626 replacing DMB as the lower axial ligand of cobalt (*25*). Therefore, we examined the effects of hATR missense mutants on the DMB-off transition. Controls showed that binding of AdoCbl to native hATR and hATR-His_8 resulted in the anticipated blue shift in the UV–visible spectrum (Figure 4A). Unexpectedly, however, binding of AdoCbl to His_8-hATR resulted in no obvious changes in the UV–visible spectrum (Figure 4B). This indicated that the N-terminal His_8 tag interfered with the ability of the hATR to mediate the base-off transition of AdoCbl. Consequently, further studies of this transition focused on variants of the hATR with the C-terminal His_8 tag.

Among the hATR missense mutants with the C-terminal His_8 tag, five mutants (S68F, K78Q, K78R, R186W, and R190C) mediated blue shifts similar to that of the wild-type hATR. However, the majority of the hATR missense mutants, including D64G, F83S, G87R, D90N, E91K, L92S, S94L, C189Y, R191W, E193K, R194G, F212S, S217R, L220P, and L223P, lacked a measurable blue shift (data not shown). The fact that most of the hATR mutants were unable to mediate the base-off transition of AdoCbl suggests that this conversion is a key aspect of the enzyme mechanism and that most of these mutations affect cobalamin binding.

Effect of Mutations on Cob(II)alamin Binding. Previous studies showed that in the presence of ATP, hATR binds

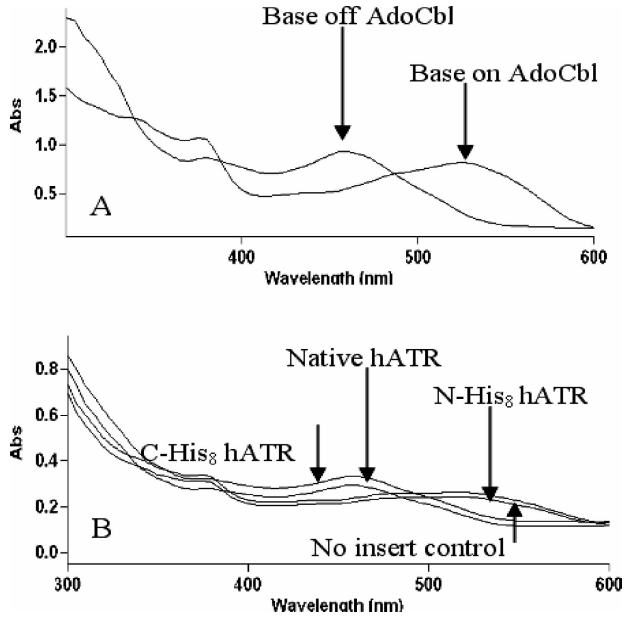

FIGURE 4: Binding of AdoCbl by hATR. UV–visible spectra of (A) AdoCbl in the base-on and base-off conformations and (B) AdoCbl bound to recombinant hATRs. One milliliter of soluble cell extract containing 10 mg of protein was scanned as the baseline. Then, AdoCbl was added to the sample and gently mixed. After incubation at 37 °C for 2 min, the cuvette was scanned a second time (shown). The strains used for hATR production were BE702 (His_8-hATR), BE704 (hATR-His_8), BE706 (native hATR), and BE119 (no insert control).

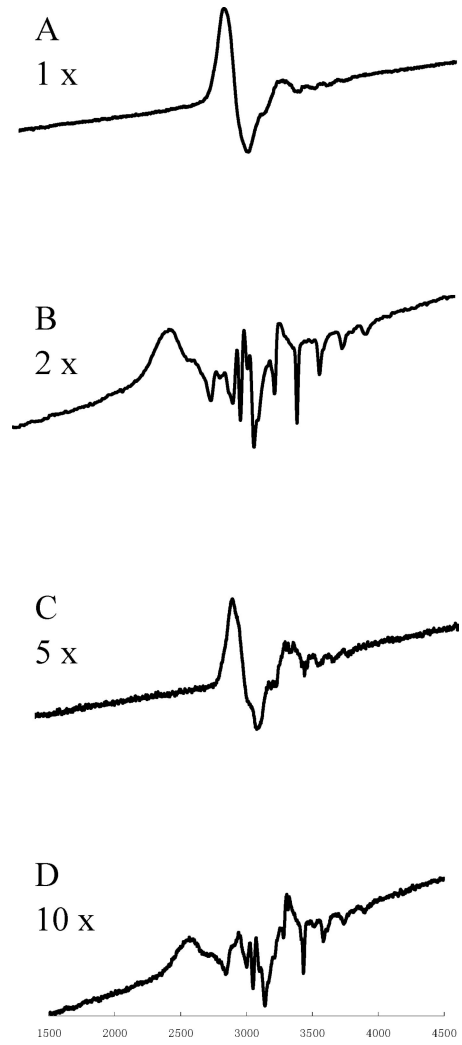

FIGURE 5: X-Band EPR spectra of (A) base-on cob(II)alamin [1 mM cob(II)alamin in 10 mM Tris-HCl buffer (pH 8.0)], (B) base-off cob(II)alamin [1 mM cob(II)alamin in 1% H_3PO_4], (C) 100 μM cob(II)alamin in the presence of 2 mM purified His_8-hATR and 2 mM ATP, and (D) 100 μM cob(II)alamin in the presence of 2 mM purified hATR-His_8 and 2 mM ATP. Spectra were collected at 100 K with a modulation amplitude of 4 G, a modulation frequency of 100 KHz, a time constant of 100 ms, and a microwave power of 20 mW.

cob(II)alamin in the base-off form (*23, 25*). Base-off binding is proposed to raise the $Co^{2+/+}$ reduction potential from −610 to −500 mV, activating the cob(II)alamin for reduction (*24*). Base-on and base-off cob(II)alamin can be distinguished by EPR spectroscopy (*23*). Base-on cob(II)alamin exhibits an EPR spectrum in which the octet of hyperfine lines is split into triplets (Figure 5A). In contrast, base-off cob(II)alamin has high-field lines that appear as singlets (Figure 5B). Therefore, we used EPR spectroscopy to examine cob(II) alamin binding by hATR and variants. Controls showed that His_8-hATR bound cob(II)alamin base-on (Figure 5C) and that hATR-His_8 bound cob(II)alamin base-off (Figure 5D). This indicated that the N-terminal His_8 tag interfered with the ability of the hATR to mediate the base-off transition of cob(II)alamin which was also seen in the case of AdoCbl binding (see above). Among the hATR missense mutants with the C-terminal His_8 tag, only S68F, K78Q, K78R, R186W, and R190C exhibited EPR spectra indicating base-off binding of cob(II)alamin (data not shown). This result was consistent with that of AdoCbl base-off transition experiments described above, suggesting that base-off binding of AdoCbl and cob(II)alamin is mechanistically related.

DISCUSSION

In this study, the hATR was subjected to random mutagenesis and an ATR-deficient *Salmonella* strain was used as a surrogate host to facilitate isolation and characterization of mutations that impaired hATR activity. This approach allowed isolation of a number of single-base change mutations that impaired hATR activity. Single-base changes are much more likely to arise in natural populations compared to two or three simultaneous base changes which are often used in site-directed mutagenesis studies. Thus, the mutations studied here are more likely to have relevance to MMA than multibase changes created by site-directed mutagenesis. In total, 57 missense mutations were found at 30 different sites of the hATR, five of which were previously shown to be altered in MMA patients and 25 of which were at new sites.

In addition to identifying mutations that have potential relevance to MMA, the studies reported here also help to functionally define the hATR active site. Analysis of hATR variants indicated that two small regions are particularly important for enzyme activity, E84−S94 and R186−R194. In the E84−S94 region, mutations in seven of 12 positions abolished enzyme activity, while in the R186−R194 region, changes in six of nine residues eliminated activity. This suggests that these two short conserved regions are part of the hATR active site which is consistent with the crystal structure determined by Schubert and Hill (*19*).

To realize a more detailed understanding of how the mutations isolated here affected hATR activity, we mapped them onto a hATR structural model with MgATP bound. The crystal shows that MgATP binding involves the formation of

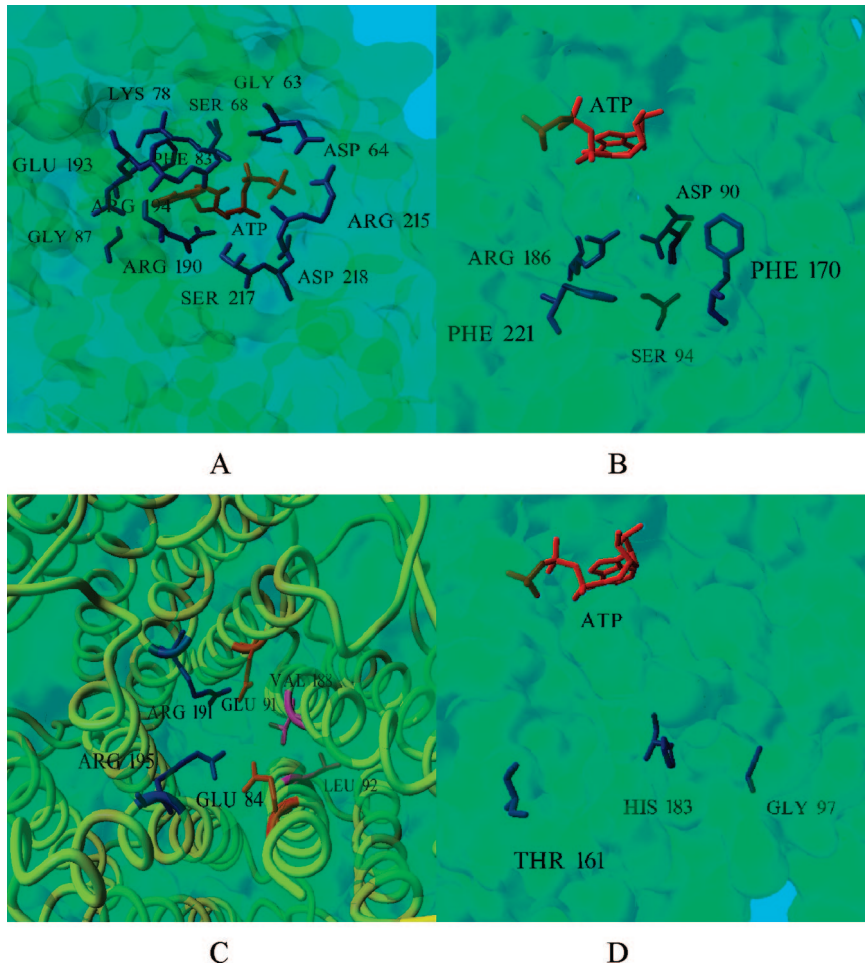

FIGURE 6: Mapping of mutations on the hATR structural model. (A) Side view of mutations involved in MgATP binding. (B) Side view of mutations at the surface of the proposed cobalamin binding site. (C) Top view of mutations at the interface of the hATR trimer. (D) Side view of mutations proposed to facilitate the base-off transition. This figure was made using Yasara.

numerous hydrogen bonds and van der Waals interactions. ATP binding also increased the order of 20 N-terminal amino acids, creating a novel ATP-binding site that was part of a larger cleft proposed to include the cobalamin binding site (*19*). Thirteen missense mutations isolated in this study affected residues directly involved in MgATP binding (G63E, D64G, S68F, K78R, K78Q, F83S, G87R, R190C, E193K, R194G, R215K, S217R, and D218N) (Figure 6A), and two missense mutations changed residues proposed to be involved in cobalamin binding (D90N and R186W). Hence, these mutations functionally define the hATR active site.

We also examined hATR mutations that resulted in an abnormal K_m value for cob(I)alamin or sensitivity to hydroxylcobalamin concentration *in vivo*. In addition to residues D90, F170, R186, and F221 which were previously suggested to aid cobalamin binding (*19*), we found that S94 sits at the inner surface of the proposed cobalamin binding site and that mutation S94L resulted in an enzyme that was inactive *in vitro* and *in vivo*, suggesting a role for S94 in cobalamin binding not apparent in the crystal structure (Figure 6B).

The crystal structure of the hATR indicates a trimer structure is required for enzyme activity since the active site is at the monomer interfaces. The trimer interface contains two charged rings (E84/R195 and E91/R191) and two phenylalanine rings that form a solid core (*19*). Among these positions, three missense mutants were obtained (E84K, E91K, and R191W). Each lacked detectable hATR activity *in vivo* and *in vitro*, indicating that these positions are likely important for trimer formation. We did not obtain mutations that alter the phenylalanine residues at the core of the trimer. However, mutant L92S (Figure 6C), which is located at the trimer interface, also lacked measurable activity *in vitro* and *in vivo*. L92 may make contact with V188 at the interface of the neighbor subunit. In addition, two mutants were obtained (L220P and L223P) that are expected to produce kinks in helix α5 which is involved in active site formation. These two mutants also lacked measurable activity *in vitro* and *in vivo*.

Recent spectroscopic studies indicate that the hATR binds cobalamin as a four-coordinate species in which DMB is no longer bonded to the central cobalt atom (*23*). This mode of binding (DMB-off) is proposed to raise the $Co^{2+/+}$ midpoint potential 110 mV (from −610 to −500 mV), bringing it into the physiological range (*24*). We found three hATR variants that had near normal activity *in vitro* but were stable and inactive *in vivo* (G97E, T161I, and H183Y). We speculate that these mutant enzymes might be unable to mediate the DMB-off transition *in vivo* and hence be inactive since formation of cob(I)alamin is a prerequisite for adenosylation. Such mutants would be expected to be inactive *in vivo* but active *in vitro* because cob(I)alamin is provided through use of a strong chemical reductant. Alternatively, mutations G97E, T161I, and H183Y might impair interaction of the hATR with a partner reductase. Studies in several systems indicate that ATRs directly interact with cognate reductases

to protect the highly reactive cob(I)alamin intermediate from side reactions (*26*–*28*). Impairment of this interaction would be expected to produce ATR that is active *in vitro* but not *in vivo* which was found for variants G97E, T161I, and H183Y. However, G97, T161, and H183 map to the interior of the hATR (Figure 6D); hence, it seems unlikely they would be able to interact with a partner protein. Therefore, we favor a possible role for G97, T161, and H183 in stabilizing four-coordinate cob(II)alamin. Each of these residues maps near a hydrophobic loop between α3 and α4 which we tentatively suggested is involved in DMB binding or otherwise facilitating cob(II)alamin reduction.

ACKNOWLEDGMENT

We thank the DNA facility of the Iowa State University Office of Biotechnology for assistance with DNA analyses. We thank the chemical instrumentation facility of Iowa State University for assistance with EPR spectroscopy. We thank Dr. Ruma Banerjee (University of Michigan, Ann Arbor, MI) and Dr. Thomas Brunold (University of Wisconsin, Madison, WI) for help with spectroscopy.

REFERENCES

1. Cauthen, S. E., Foster, M. A., and Woods, D. D. (1966) Methionine synthesis by extracts of *Salmonella typhimurium*. *Biochem. J. 98*, 630–635.
2. Matthews, R. G. (1999) Cobalamin-dependent methionine synthase, in *Chemistry and Biochemistry of B12* (Banerjee, R., Ed.) pp 681–707, John Wiley & Sons, Inc., New York.
3. Banerjee, R., and Chowdhury, S. (1999) Methylmalonyl-CoA mutase, in *Chemistry and Biochemistry of B12* (Banerjee, R., Ed.) pp 707–730, John Wiley & Sons, Inc., New York.
4. Banerjee, R. (2006) B_{12} trafficking in mammals: A case for coenzyme escort service. *ACS Chem. Biol. 1*, 149–159.
5. Vitols, E., Walker, G. A., and Huennekens, R. M. (1966) Enzymatic conversion of vitamin B_{12s} to a cobamide coenzyme, α-(5,6-dimethylbenzimidazolyl)deoxyadenosylcobamide (adenosyl-B_{12}). *J. Biol. Chem. 241*, 1455–1461.
6. Weissbach, H., Redfield, B., and Peterkofsky, A. (1961) Conversion of vitamin B_{12} to coenzyme B_{12}in cell-free extracts of *Clostridium tetanomorphum*. *J. Biol. Chem. 236*, PC40–PC42.
7. Fujii, K., Galivan, J. H., and Huennekens, F. M. (1977) Activation of methionine synthase: Further characterization of flavoprotein system. *Arch. Biochem. Biophys. 178*, 662–670.
8. Fujii, K., and Huennekens, F. M. (1974) Activation of methionine synthetase by a reduced triphosphopyridine nucleotide-dependent flavoprotein system. *J. Biol. Chem. 249*, 6745–6753.
9. Rosenblatt, D. S., and Fenton, W. A. (1999) Inborn errors of cobalamin metabolism, in *Chemistry and Biochemistry of B12* (Banerjee, R., Ed.) pp 367–384, John Wiley & Sons, Inc., New York.
10. Watkins, D., and Rosenblatt, D. S. (2001) Cobalamin and inborn errors of cobalamin absorption and metabolism. *Endocrinologist (Hagerstown, MD, U.S.) 11*, 98–104.
11. Fenton, W. A., Gravel, R. A., and Rosenblatt, D. (2000) Disorders of propionate and methylmalonate metabolism, in *The Metabolic and molecular basis of inherited disease* (Scriver, C. R., Beaudet, A. L., Sly, W. S., Valle, D., Childs, B., Kinzler, K. W., and Vogelstein, B., Eds.) McGraw-Hill, New York.
12. Brady, R. O., Castanera, E. G., and Barker, H. A. (1962) The enzymatic synthesis of cobamide coenzymes. *J. Biol. Chem. 237*, 2325–2332.
13. Johnson, C. L. V. J., Pechonick, E., Park, S. D., Havemann, G. D., Leal, N. A., and Bobik, T. A. (2001) Functional genomic, biochemical, and genetic characterization of the *Salmonella* pduO gene, an ATP:cob(I)alamin adenosyltransferase gene. *J. Bacteriol. 183*, 1577–1584.
14. Buan, N. R., Suh, S. J., and Escalante-Semerena, J. C. (2004) The *eutT* gene of *Salmonella enterica* encodes an oxygen-labile, metal-containing ATP:corrinoid adenosyltransferase enzyme. *J. Bacteriol. 186*, 5708–5714.
15. Sheppard, D. E., Penrod, J. T., Bobik, T., Kofoid, E., and Roth, J. R. (2004) Evidence that a B_{12}-adenosyl transferase is encoded within the ethanolamine operon of *Salmonella enterica*. *J. Bacteriol. 186*, 7635–4644.
16. Escalante-Semerena, S. S., and Roth, J. R. (1990) *cobA* function is required for both de novo cobalamin biosynthesis and assimilation of exogenous corrinoids in *Salmonella typhimurium*. *J. Bacteriol. 172* (1), 273–280.
17. Leal, N. A., Park, S. D., Kima, P. E., and Bobik, T. A. (2003) Identification of the human and bovine ATP:cob(I)alamin adenosyltransferase cDNAs based on complementation of a bacterial mutant. *J. Biol. Chem. 278*, 9227–9234.
18. Dobson, C. M., Wai, T., Leclerc, D., Kadir, H., Narang, M., Lerner-Ellis, J. P., Hudson, T. J., Rosenblatt, D. S., and Gravel, R. A. (2002) Identification of the gene responsible for the *cblB* complementation group of vitamin B_{12}-dependent methylmalonic aciduria. *Hum. Mol. Genet. 11*, 3361–3369.
19. Schubert, H. L., and Hill, C. P. (2006) Structure of ATP-Bound Human ATP:Cobalamin Adenosyltransferase. *Biochemistry 45* (51), 15188–15196.
20. St Maurice, M. M. P., Taranto, M. P., Sesma, F., Escalante-Semerena, J. C., and Rayment, I. (2007) Structural characterization of the active site of the PduO-type ATP:Co(I)rrinoid adenosyltransferase from *Lactobacillus reuteri*. *J. Biol. Chem. 282* (4), 2596–2605.
21. Saridakis, V., Yakunin, A., Xu, X., Anandakumar, P., Pennycooke, M., Gu, J., Cheung, F., Lew, J. M., Sanishvili, R., Joachimiak, A., Arrowsmith, C. H., Christendat, D., and Edwards, A. M. (2004) The structural basis for methylmalonic aciduria: The crystal structure of archeael ATP:cobalamin adenosyltransferase. *J. Biol. Chem. 279* (22), 23646–23653.
22. Bauer, C. B., Fonseca, M. V., Holden, H. M., Thoden, J. B., Thompson, T. B., Escalante-Semerena, J. C., and Rayment, I. (2001) Three-dimensional structure of ATP:corrinoid adenosyltransferase from *Salmonella typhimurium* in its free state, complexed with MgATP, or complexed with hydroxycobalamin and MgATP. *Biochemistry 40*, 361–374.
23. Stich, T. A., Yamanishi, M., Banerjee, R., and Brunold, T. C. (2005) Spectroscopic evidence for the formation of a four-coordinate Co^{2+} cobalamin species upon binding to the human ATP:cobalamin adenosyltransferase. *J. Am. Chem. Soc. 127* (21), 7660–7661.
24. Doris Lexa, J.-M. S. (1983) The Electrochemistry of Vitamin B_{12}. *Acc. Chem. Res. 16*, 235–243.
25. Yamanishi, M. L. T., and Banerjee, R. (2005) Mirror "base-off" conformation of coenzyme B_{12} in human adenosyltransferase and its downstream target, methylmalonyl-CoA mutase. *J. Am. Chem. Soc. 127* (2), 526–527.
26. Buan, N. R., and Escalante-Semerena, J. C. (2005) Computer-assisted docking of flavodoxin with the ATP:Co(I)rrinoid adenosyltransferase (CobA) enzyme reveals residues critical for protein-protein interactions but not for catalysis. *J. Biol. Chem. 280* (49), 40948–40956.
27. Sampson, J. C., and Bobik, T. A. (2005) Biochemical evidence that the *pduS* gene encodes a bifunctional cobalamin reductase. *Microbiology 15*, 1169–1177.
28. Leal, N. A., Olteanu, H., Banerjee, R., and Bobik, T. A. (2004) Human ATP:cob(I)alamin adenosyltransferase and its interaction with methionine synthase reductase. *J. Biol. Chem. 279* (46), 47536–47542.
29. Schrauzer, G. N., Deutsch, E., and Windgassen, R. J. (1968) The nucleophilicity of vitamin B_{12}. *J. Am. Chem. Soc. 90*, 2441–2442.
30. Johnson, C. L., Buszko, M. L., and Bobik, T. A. (2004) Purification and initial characterization of the *Salmonella enterica* PduO ATP: Cob(I)alamin adenosyltransferase. *J. Bacteriol. 186*, 7881–7887.
31. Zhang, J. D. C., Wu, X., Lerner-Ellis, J., Rosenblatt, D. S., and Gravel, R. A. (2006) Impact of cblB mutations on the function of ATP:cob(I)alamin adenosyltransferase in disorders of vitamin B_{12} metabolism. *Mol. Genet. Metab. 87* (4), 315–322.
32. Bobik, T. A., and Wolfe, R. S. (1989) Activation of formylmethanofuran synthesis in cell extracts of *Methanobacterium thermoautotrophicum*. *J. Bacteriol. 171*, 1423–1427.
33. Maniatis, T., Fritsch, E. F., and Sambrook, J. (1982) *Molecular Cloning: A Laboratory Manual*, Cold Spring Harbor Laboratory Press, Plainview, NY.
34. Jeter, R. M. (1990) Cobalamin-dependent 1,2-propanediol utilization by *Salmonella typhimurium*. *J. Gen. Microbiol. 136*, 887–896.

BI800084A